

Adsorption isotherm and kinetic studies for the decolorization of sunset yellow FCF dye using economically feasible low-cost adsorbent

M.N. Nafisa Begam^{1*}, K. Muthukumaran², P. Thamarai³ and J Prince Joshua⁴

^{1*}Department of Industrial Biotechnology, Government College of Technology, Coimbatore-641013.

²Department of Chemistry, Government College of Technology, Coimbatore-641013.

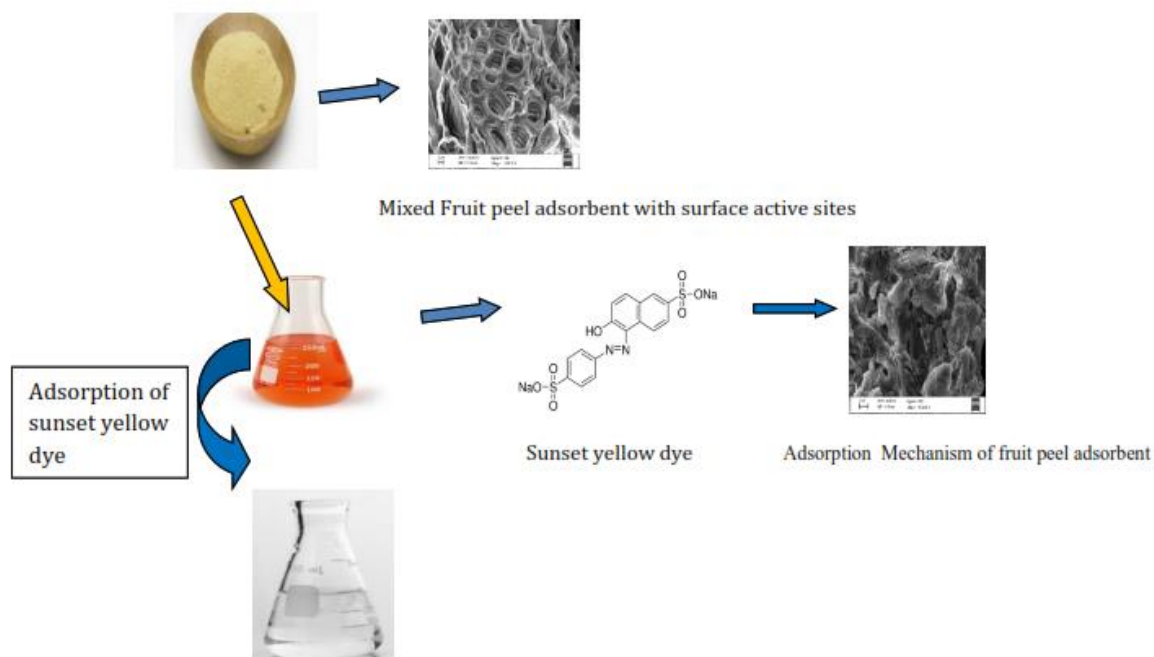
³Department of Environmental Engineering, Government College of Technology, Coimbatore-641013.

⁴Department of Physics, The New College (Autonomous), Chennai – 600014

*Corresponding author:

Email: nafisa.mn.ibt@gct.ac.in Phone: +91-94435-48646.

Graphical abstract:



22

23 **ABSTRACT**

24 The present communication attempts to explore the adsorption potential of Mixed Fruit Peel
25 Waste (MFPW) to remove Sunset Yellow FCF dye from an aqueous solution. The MFPW is a low-
26 cost adsorbent prepared from the peels orange, watermelon and banana. The characterization of
27 MFPW was made through FTIR, SEM and BET studies. The FTIR studies revealed the presence of
28 functional groups such as nitro, carboxyl, ester, ether, phenol and alkyne that are solely responsible
29 for adsorption. The surface morphology exposed the clear and well-developed pores of MFPW.
30 Batch adsorption studies resulted in a maximum adsorption capacity (q_{\max}) of 200 mg/g at optimum
31 pH 3.0, contact time of 100 minutes, and adsorbent dose of 2.0 g/L with an initial dye concentration
32 of 40 ppm. Sunset Yellow FCF dye removal was discovered to be spontaneous and endothermic in
33 nature, with the Langmuir isotherm and pseudo-second-order-kinetics providing the best fit. In
34 summary, mixed fruit peel waste adsorbent can be used as a low-cost, environmentally friendly and
35 sustainable adsorbent to decolorize sunset yellow FCF dye.

36 **Keywords:** Adsorption, sunset yellow, mixed fruit peel waste adsorbent.

37

38 **1. Introduction**

39 Dye effluents are released during the dyeing process in the textile, food, printing, leather,
40 plastic, and cosmetic industries [Hejun Gao *et al.*, 2013, Yu Zhiyong *et al.*, 2013]. These dye
41 effluents have an impact on groundwater quality by altering parameters like Biological Oxygen
42 Demand (BOD), Chemical Oxygen Demand (COD), Total Organic Solids (TOS), Total Dissolved
43 Solids (TDS), and Total Suspended Solids (TSS) [Garba, Z.N *et al.*, 2019, Xiaoduo Liu *et al.*,
44 2019]. It is also known that dye effluents cause eutrophication (the blocking of sunlight), depleting
45 nutrients in the water and endangering aquatic life. Nonetheless, consuming such polluted water has
46 a significant impact on terrestrial life, resulting in serious health issues such as asthma, cancer, skin

47 and throat irritation, and so on. As a result, proper treatment of dye effluents from industries has
48 become critical [Rangabhashiyam S *et al.*, 2017].

49 There are currently several treatment options available, including filtration, precipitation,
50 membrane separation, ion exchange, coagulation, flocculation, and adsorption, with the adsorption
51 method being versatile, cost-effective and ease of operation [Jayalakshmi and Jeyanthi 2021;
52 Zhifeng Jiang *et al.*, 2014, Yonggang Liu *et al.*, 2010]. Researchers have developed various
53 adsorbents to remove dye effluents from the environment, such as activated carbon, sawdust,
54 bagasse fly ash, guava seeds, nanocomposites, lignocellulosic biomass, and agricultural byproducts
55 such as fruit peels, wheat, and rice bran. But many adsorbents fail to meet the minimum
56 requirements for wastewater recycling, such as high selectivity and good adsorption capacity for
57 wastewater recycling [Garg VK *et al.*, 2003; Mall, Indra D *et al.*, 2006]. However, due to its high
58 adsorption capacity, various fruit waste has been highlighted as an adsorbent in previous studies
59 [Husseien, M *et al.*, 2007; Ranjithkumar.V *et al.*, 2017].

60 Among other adsorbents, fruit waste adsorbents are cost-effective, sustainable,
61 biocompatible, easy to scale up and environmentally friendly, making them a promising candidate
62 for wastewater treatment. Moreover, water material utilization can bridge the gap between the
63 water-energy-food circular economies [Hossain *et al.*, 2020; Solangi *et al.*, 2021]. Previous research
64 has shown that noncarbonized guava seeds effectively adsorb selective azo and anthraquinone dyes.
65 Similarly, Methylene Blue, Eriochrome Black T, and Alizarin S dyes can be removed using dried
66 prickly pear cactus cladodes adsorbent [Barka, Nouredine *et al.*, 2009, A. Machrouhi *et al.*, 2017].
67 The peels of *Punica granatum L.* were found to adsorb 98.07 % of Pb (II) ions and 94.76 % of Acid
68 Blue 40 from industrial wastewaters. Rhodamine B and Methylene Blue were removed using
69 digested fruit waste [Hussain, Sajjad *et al.*, 2016, Bhatnagar, Amit *et al.*, 2009].

70 The adsorbent behavior of mixed fruit biomass for removing dyes in the literature was
71 insignificant so far. However, the effectiveness of activated carbon derived from fruit waste as an
72 adsorbent was reported in many studies [Wong *et al.*, 2018; Sahu *et al.*, 2020; Ramalingam *et al.*,

2020]. Moreover, the studies reported that biomass could be a potential substitute for activated carbon, reducing operational costs [Rebitanim *et al.*, 2012]. Therefore, an attempt was made to prepare mixed fruit peel waste biomass cost-effectively and efficiently, without chemical or thermal activation in this study. Furthermore, its corresponding adsorptive behavior for dye removal was studied. Moreover, the reported adsorption capacity of mixed fruit peel waste is higher when compared to other fruit waste as well as activated carbons [Lim *et al.*, 2020; Nguyen *et al.*, 2020].

This study investigates the utilization of mixed fruit peel (orange, watermelon, and banana waste peels) as adsorbents for removing sunset yellow FCF dye. First, the mixed fruit peel waste adsorbent's morphology and chemical properties are well-characterized using FTIR spectroscopy and SEM analysis. Then, batch adsorption studies were conducted to assess its adsorptive behavior for sunset yellow FCF dye from an aqueous solution. And the biosorption efficiency of mixed fruit peel waste adsorbent is evaluated by optimizing the effects of pH, contact time, adsorbent dosage, initial dye concentrations and temperature. Finally, the results from the batch adsorption studies were validated using isotherm, kinetics, and thermodynamic studies.

2. Experimental Set up:

2.1. Methods and Materials

This study only used analytical-grade chemical reagents. The Sunset Yellow FCF (SY FCF) textile dye was purchased from Sigma-Aldrich and used without further purification. Deionized water was used to prepare the Sunset yellow dye stock solution, then used to prepare various concentrations of solutions. The pH was adjusted with a solution of HCl and NaOH. Each experiment necessitated the use of brand-new dilutions. Orange, watermelon, and banana peels were purchased from a nearby juice shop and washed in deionized water. They were finely chopped into small pieces to make crushing easier. The peels were kept in a hot air oven at 70°C for 48 hours. After drying, the pieces were ground into a fine powder in a mixer grinder and sieved through a 150 μm mesh sieve to obtain uniformly sized particles. Finally, the powdered mixed fruit

98 peel waste was stored in an airtight container for future use. [Bhatnagar, Amit *et al.*, 2021,
99 Khaskheli M.I *et al.*, 2021]

100 **2.2. Characterization of prepared adsorbent**

101 FTIR spectra were used to investigate the chemical functional groups of the adsorbent, and
102 the adsorbent was loaded as KBr discs and recorded in a Fourier Transform Infrared
103 Spectrophotometer (PerkinElmer Spectrum Two). A surface area analyzer was used to investigate
104 mixed fruit peel waste's pore size, surface area, and pore volume (BELSORP-Mini II). The
105 adsorbent's surface morphology was investigated using a scanning electron microscope (ZEISS). A
106 UV-Visible spectrophotometer (Systronics) was used to measure the absorption of sunset yellow
107 dye ($\lambda_{max} = 482$ nm). The pH of the aqueous solutions was determined using a Labman model pH
108 metre with a glass electrode [Ahmad, M. A *et al.*, 2021, Almeida-Naranjo, C. E *et al.*, 2021].

109 **2.3. MFPW point of zero charge determination**

110 The salt addition method was used to determine the adsorbent's net neutral charge. Using 0.1M
111 HCl/NaOH, the initial pH of the 0.1M potassium nitrate solutions was set in the range of 2.0 – 10.0.
112 0.1 g of MFPW adsorbent was added and agitated at 120 rpm for 24 hours. The final pH of the
113 solution was recorded. The zero-point charge of the adsorbent was determined by drawing a graph
114 between Δ pH and initial pH [Solangi, N. H *et al.*, 2021].

116 **2.4. Biosorption experiments**

117 Batch adsorption studies using mixed fruit peel waste powder were carried out to optimize
118 process parameters such as pH, contact time, adsorbent dosage, initial dye concentration and
119 temperature. The pH was adjusted with HCl and NaOH, and residual concentrations were
120 determined using a standard graph in a UV-Visible spectrophotometer. The experiments were
121 carried out with a stock dye solution containing 20mg/L of SY-FCF, and parameters such as contact
122 time (5.0 – 200 minutes), adsorbent dosages (0.5-2.0g), and pH were varied (3-10).

123 **2.5. Isotherm and kinetic studies**

Two grams of adsorbent were used in a series of conical flasks with initial dye concentrations (10-50mg/L) at pH 3.0 for adsorption equilibrium studies. In a rotary orbital shaker (Scigenics), the flasks were incubated for 60 minutes at 120 rpm. The concentration of the treated SY FCF dye solution was determined at 482nm using a UV-Visible spectrophotometer after the adsorbent was removed from the supernatant. The equilibrium adsorption rate (q_e) was given in equation 1, and the percentage of dye removal was calculated from equation 2:

$$q_e = \frac{(C_0 - C_e) * V}{m} \quad (1)$$

where q_e (mg/g) is defined as the quantity of dye adsorbed per unit mass of adsorbent, C_0 & C_e are initial and final dye concentration (mg/L), V is the volume of the SY FCF dye solution and m is the mass of the adsorbent, respectively [Gupta, Shubham A *et al.*, 2021]. Meanwhile, Removal efficiency is calculated as follows.

$$\% \text{ Removal} = \frac{(C_0 - C_e)}{C_0} * 100 \quad (2)$$

3. Results and Discussion

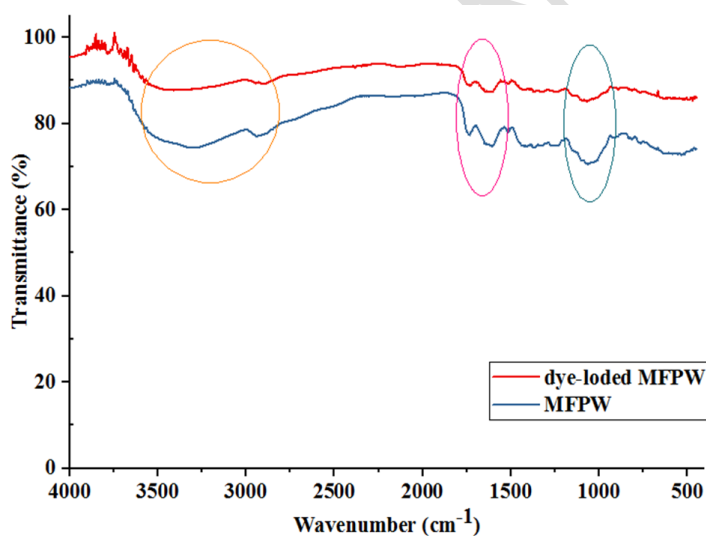
3.1. Characterisation of adsorbent

FTIR Studies

FTIR peak of the MFPW adsorbent before and after adsorption (Fig. 1) was evaluated to identify the functional groups responsible for SY FCF adsorption.

Fig. 1: FTIR spectra of MFPW and dye-loaded MFPW

Table 1: Different functional groups identified by FTIR spectra before and after adsorption.



Functional group	Before adsorption Wavenumber(cm^{-1})	After adsorption Wavenumber(cm^{-1})
O-H stretching of hydroxyl group	3787.72	3637.18
C-C stretching of alkyne group	2937.82	-
C-O stretching vibrations in quinine structure	1610.12	1605.59
C-O group stretching in ester, ether or phenol groups	1243.79	1237.17
C-N stretching of aliphatic primary amines	1065.35	1069.47
CH_3 or CH_2 groups bending vibration in carboxylic acid	1369.76-1578.51	-

C-H bending in functional group	535.29	470.78-672.44
---------------------------------	--------	---------------

Table 1 shows the FTIR spectrum of MFPW and dye-loaded MFPW. The adsorption capacity may be affected by the chemical reactivity of the surface functional group. The fruit peel comprises cellulose and pectin, and signals corresponding to O-H, C-O, C-H, and C-C bonds were found. After adsorption, the peaks at 2937.82cm^{-1} and $1300\text{-}1600\text{cm}^{-1}$ vanish, indicating that the C-C stretching of the alkyne group and C-H bending in a carboxylic acid functional group is responsible for SY FCF adsorption onto MFPW [Idris, Mohd Nazri *et al.*, 2011; Sun, Yong *et al.*, 2010]. Furthermore, the rest of the peaks in MFPW have shifted to lower intensity after the SYFCF adsorption onto MFPW. Adsorption is attributed to functional groups such as nitro, carboxyl, ester, ether, phenol, and alkyne groups.

Surface Morphology:

a)

b)

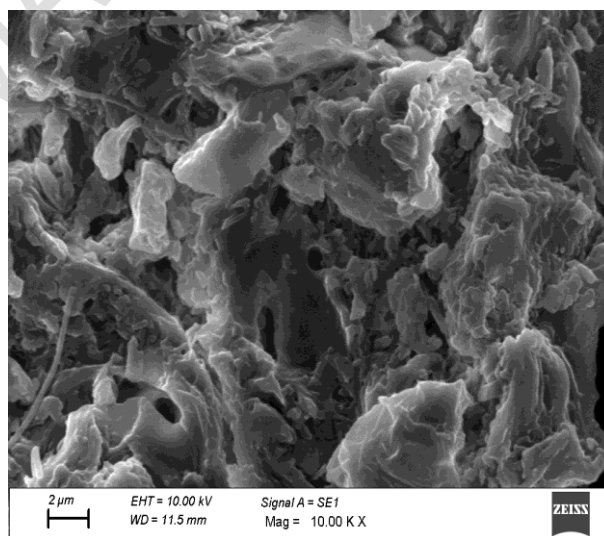
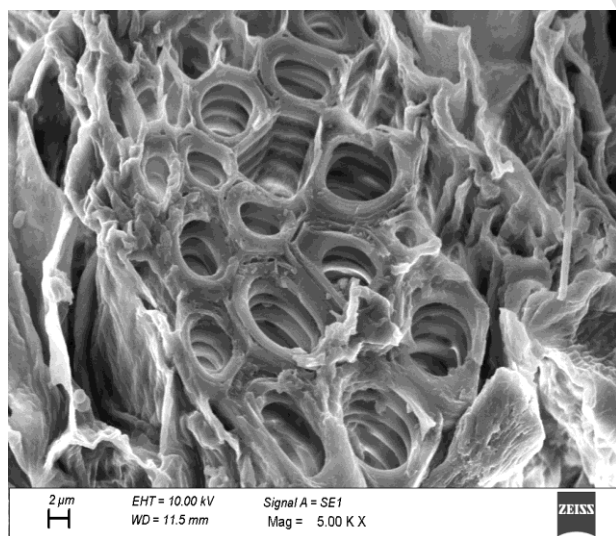


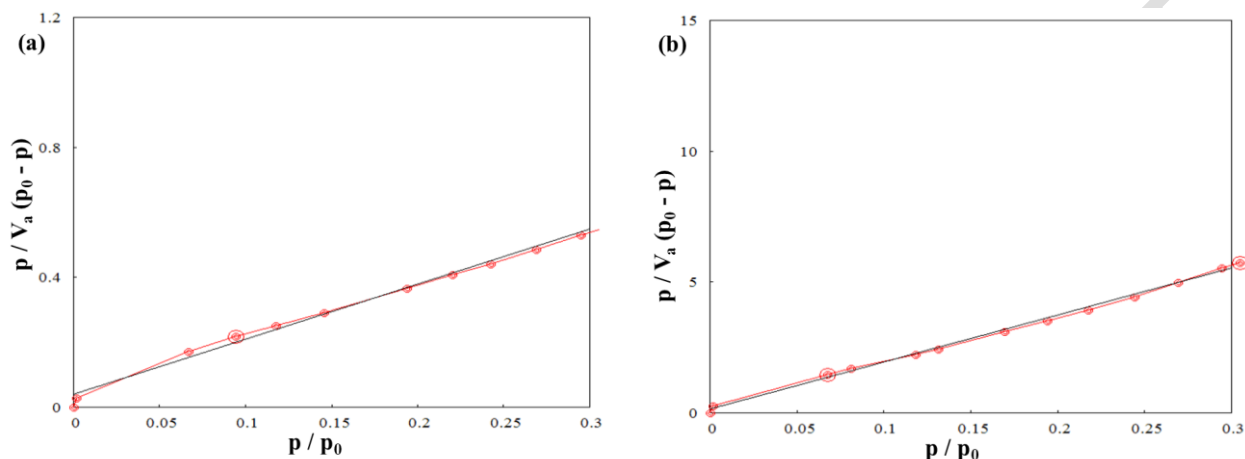
Fig. 2: SEM micrograph of MFPW and dye-loaded MFPW

Before and after SY FCF adsorption, the surface morphology of the mixed fruit peel waste was observed at $2\text{ }\mu\text{m}$ magnification of the adsorbent. Fig. 2(a) showed that the surface morphology is clear and has well-developed pores. The pore development could be due to the activation of pores during thermal expansion. These pores allow dye molecules to come and sit on its. Therefore, the MFPW's adsorption capacity may be influenced by the pore size and pore

174 volume of adsorption sites to accumulate a more significant number of dye molecules. [Auta, M *et*
 175 *al.*, 2011; Aksu, Z *et al.*, 2010; Shoukat, Sidra *et al.*, 2017]. Fig. 2(b) shows that the surface of
 176 MFPW was covered with dye molecules.

177

178



179

180 **Fig. 3: BET studies for MFPW and dye-loaded MFPW**

181 The MFPW was investigated using N₂ adsorption/desorption isotherm studies to study the
 182 porosity and surface area. And the corresponding BET plot was depicted in Fig. 3. The MFPW's
 183 surface area, total pore volume, and mean pore diameter before and after adsorption were found to
 184 be 2.5 m²/g, 0.0045cm³/g, 7.25nm, and 0.2 m²/g, 0.00024cm³/g, 4.06nm, respectively. It is
 185 understood that raw adsorbents have a larger surface area and pore volume, indicating that the
 186 adsorption cavities are receptive to dye molecules. Furthermore, the values in the recovered
 187 adsorbents are reduced following the adsorption studies. This corresponds to the BET surface area
 188 of *P. granatum L.* peels [16]. The surface area and pore diameter of the adsorbent are highly
 189 dependent on the adsorption sites, which are highly advantageous for effective dye adsorption.
 190 Since the mixture of fruit peel waste has a different surface area, the dye molecules can easily attach
 191 to the adsorption site, which can be predicted using the sample's pore volume [Idris, Mohd Nazri *et*
 192 *al.*, 2011].

193 3.2. Point of Zero charge and effect of pH

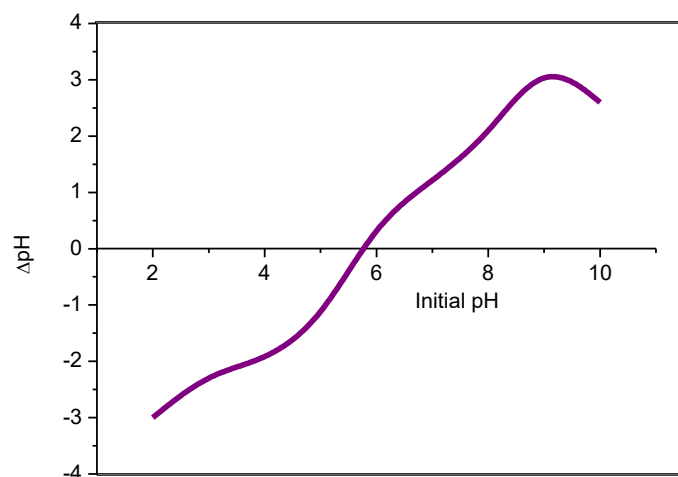


Fig. 4: P_{ZPC} of the biosorbent

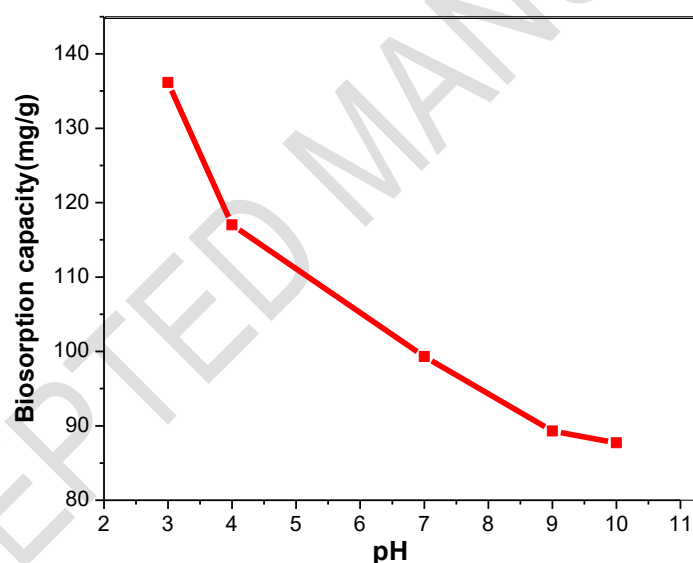


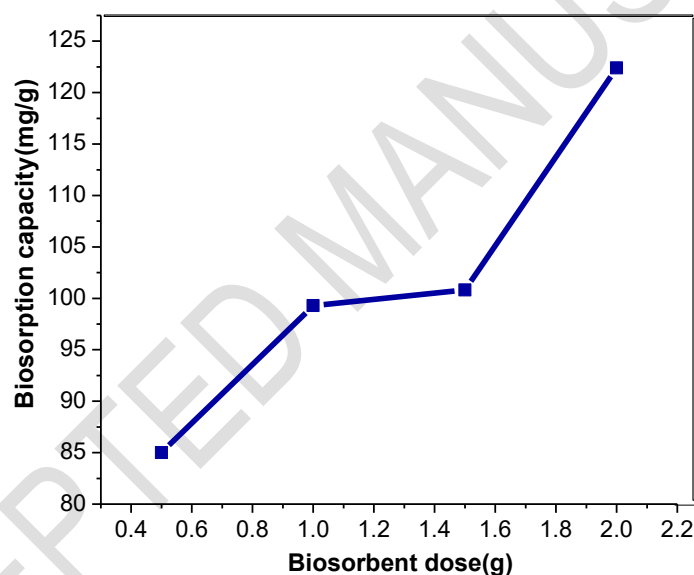
Fig. 5: Effect of pH for the adsorption of sunset yellow dye using MFPW adsorbent

Fig. 5 shows the effect of pH on SY FCF adsorption using mixed fruit peel waste. And the adsorption was conducted with initial concentration 50mg/L, shaking speed 120rpm, adsorbent dose 2.0 g/100mL, pH 3-10, contact time 120 mins, temperature 30°C.

MFPW biosorbent was discovered to have a P_{ZPC} of nearly 5.9, as shown in Fig. 4. As a result, pH levels above and below 5.9 may be optimal for dye adsorption. Because the proteins and amino acids in the mixed fruit peel waste are easily ionised in dye solutions, they affect the charged

204 surface of the adsorbent [Aksu, Z *et al.*, 2010; Shoukat, Sidra *et al.*, 2017]. Pzpc of the biosorbent is
 205 more positively charged at acidic pH, making it more attractive for the adsorption of sunset yellow,
 206 which belongs to the anionic dyes. Because hydroxyl ions are present, pH above 5.9 is negatively
 207 charged, allowing anions to be repelled under these conditions. The biosorption of an anionic dye
 208 sunset yellow was found to be optimal at pH 3.0, indicating that positively charged ions on the
 209 surface of an adsorbent are favourable for anion attraction, as demonstrated by the results of this
 210 study. The adsorption capacity of sunset yellow dye was measured at 136.16mg/g at pH 3.0 and
 211 gradually decreased to 87.7mg/g at pH 10.

212 3.3. Effect of biosorbent loading:



213
 214 **Fig. 6: Effect of biosorbent dose for the adsorption of sunset yellow dye using MFPW**
 215 **adsorbent**

216 Fig.6 shows the effect of MFPW dose on SY FCF removal. The experiments were
 217 conducted under the conditions of pH 3.0, initial dye concentration 50mg/L, shaking speed 120rpm
 218 and adsorbent dose 0.5-2g/100ml) for 120 minutes at 30°C.

219 The biosorbent dose is regarded as a critical parameter in the process for ensuring the
 220 viability of the adsorption process. The MFPW adsorbent doses ranged from 0.5 to 2.0 g/100mL.
 221 Initially the experiment was carried out with a dye concentration of 50 mg/L at pH 3.0. Sunset

222 yellow dye adsorption required 2.0g of mixed fruit peel waste due to the large number of surface
 223 adsorption sites [Shoukat, Sidra *et al.*, 2017]. Therefore, the percentage removal of dye was slightly
 224 increased between 0.5 and 1.5 g/100 mL of dye solution because there were fewer adsorption sites.
 225 Still, it reached its maximum at 1.5-2.0 g/100 mL of dye solution due to the large number of active
 226 sites on its surface, as shown in Fig. 6. As a result, biosorbent dose of up to 2.0 g/100mL is
 227 recommended for future experiments.

228 **3.4. Effect of initial dye concentration and biosorption isotherms:**

229 Langmuir, Freudlich, Temkin, Dubinin-Radushkevich and Harkins -Jura adsorption
 230 isotherm model to study the adsorption of Sunset Yellow FCF dye onto mixed fruit peel waste
 231 adsorbent.

232 Langmuir isotherm model is represented by the equation 3

$$233 \quad \frac{C_e}{q_e} = \frac{1}{bq_{\max}} + \frac{C_e}{q_{\max}} \quad (3)$$

234 Where C_e (equilibrium concentration), q_e (adsorption capacity), q_m (Langmuir maximum adsorption
 235 capacity). The Langmuir constants q_m and K_L are calculated from the slope and intercept of linear
 236 plot between C_e/q_e vs C_e .

237 The linear form of Freundlich isotherm model is given by equation 4

$$238 \quad \log q_e = \log K_f + \frac{1}{n} \log C_e \quad (4)$$

240 The plot between Log q_e versus Log C_e provides the slope $1/n$ and the intercept K_f in the
 241 graph. K_f is the Freundlich constant, and n is the exponent of the Freundlich number.

242 Equation 5 represents the Temkin isotherm model in its non-linear form.

$$\frac{X}{m} = B \ln A + B \ln C_e \quad (5)$$

Where, B_T denotes the Temkin isotherm constant related to the heat of biosorption (KJ/mol). A_T represent Temkin isotherm equilibrium binding constant (L/g).

Dubinin-radushkevich isotherm model is given by Equation.6

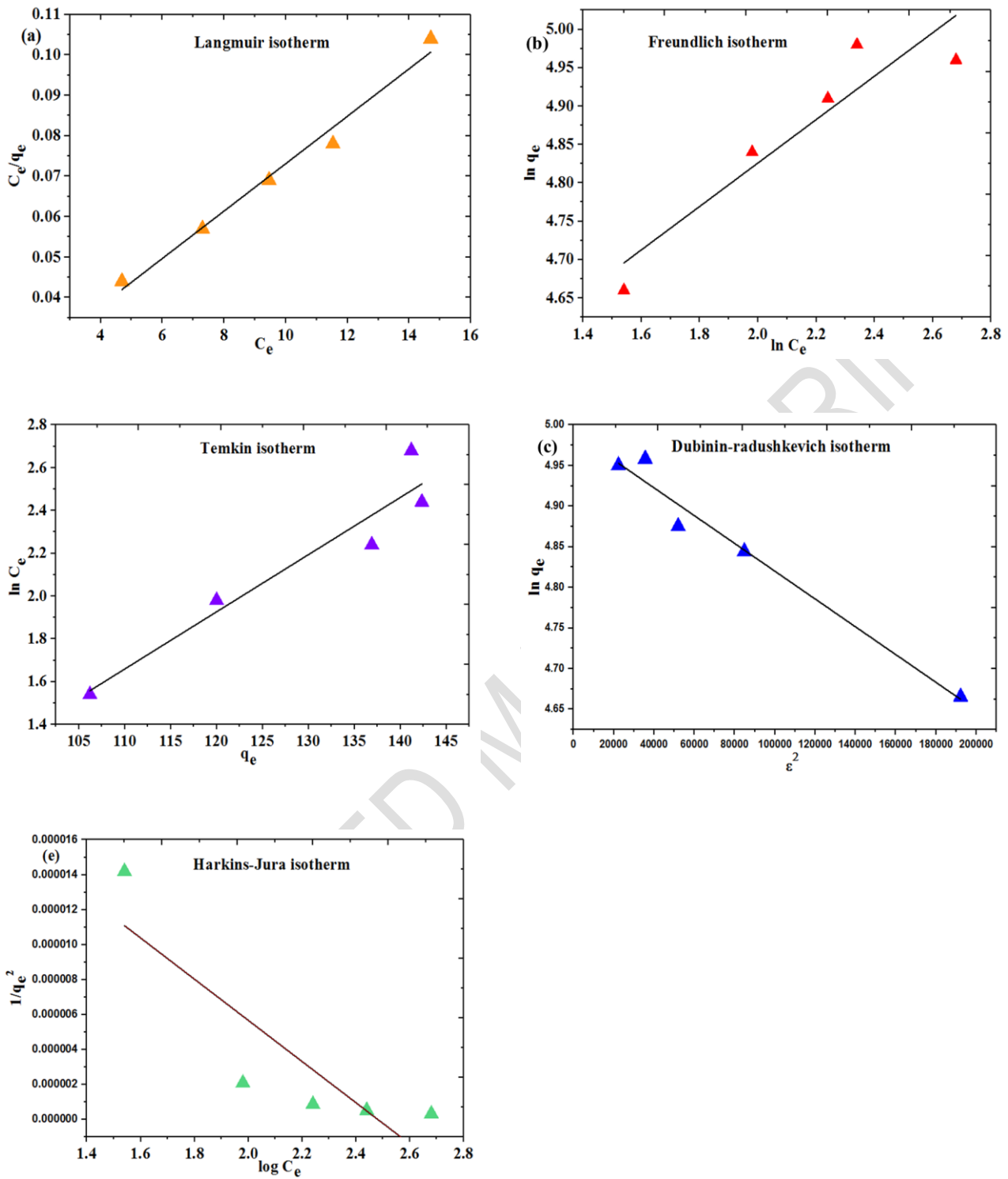
$$\ln q_e = \ln q_D - B_D (\varepsilon)^2 \quad (6)$$

where ε represents the mean free energy of adsorption (kJ/mol) can be determined by using Equation 7

$$\varepsilon = RT \ln \left(1 + \frac{1}{C_e} \right) \quad (7)$$

Harkins -Jura isotherm investigates the multilayer adsorption model and it accounts for the heterogenous pore distribution phenomenon. It is represented in Equation 8

$$\frac{1}{q_e^2} = \frac{B}{A} - \frac{1}{A \log C_e} \quad (8)$$



259 Fig. 7: (a) - Langmuir isotherm plot; (b) Freundlich isotherm plot; (c) Temkin isotherm plot; (d)
 260 Dubinin Radushkevich isotherm; (e) Harkins - Jura isotherm plot for the removal of sunset yellow
 261 dye.

262 Fig. 7 shows the isotherm plots for SYFCF adsorption onto MFPW and their corresponding
 263 kinetic parameters and regression coefficients are presented in Table 2. From Table 2, the higher
 264 order of regression coefficient follows: Langmuir > DR > Freundlich > Temkin > HJ isotherm.

265 There was an indication of chemical adsorption if free mean energy (E) was between 8 and 16
 266 kJ/mol. According to the literature, in this study, the free energy value of 0.5kJ/mol is lower than 8
 267 kJ/mol. Hence, it is understood that this might be due to electrostatic or van der Waals interactions,
 268 and the adsorption of sunset yellow FCF dye onto MFPW adsorbent was concluded to be a
 269 physisorption process. Based on regression coefficients of 0.99, it can be concluded that the
 270 Langmuir isothermal model showed the best fit with a maximum adsorption capacity of 200 mg/g
 271 for adsorption of sunset yellow FCF dye onto MFPW.

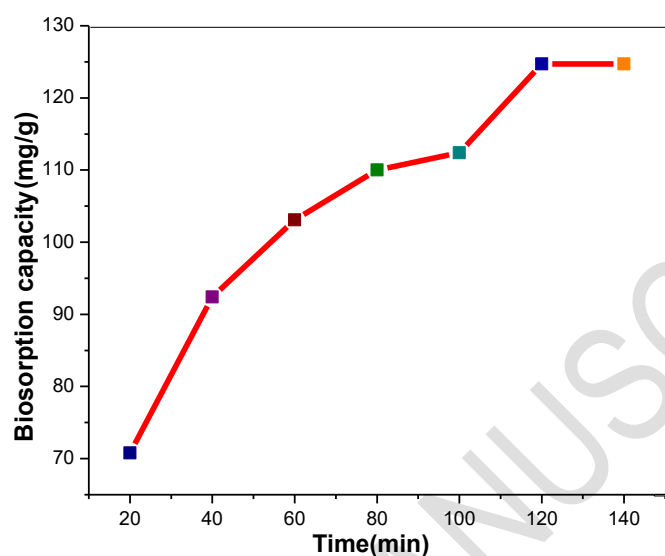
272 **Table 2: Estimated constants of Langmuir, Freundlich, Temkin, Dubinin–Radushkevich and**
 273 **Harkins-Jura isotherms for adsorption of sunset yellow dye.**

Isotherm	Parameters	Values
Langmuir	q_m (mg g ⁻¹)	200
	$B(Lmg^{-1})$	0.35
	R^2	0.99
Freundlich	K_F	71.88
	N	3.70
	R^2	0.925
Temkin	A (L g ⁻¹)	6.296
	RT/b_T	32.53
	R^2	0.90
Dubinin–Radushkevich	q_s (mg/g)	5.004
	k_{ad} (mol ² /J ²)	2×10^{-6}
	E (kJ/mol)	0.5
	R^2	0.989
Harkins – jura isotherm	A	1×10^5
	B	3×10^{10}

	R^2	0.752
--	-------	-------

274

275 3.5. Effect of contact time and kinetic studies:



276

277 **Fig. 8: Effect of contact time for the adsorption of sunset yellow dye using MFPW adsorbent**

278 Fig.8 shows the effect of contact time for SY FCF dye adsorption onto MFPW. And the
 279 experiments were conducted at varying contact with pH 3.0, 50mg/L of initial dye concentration,
 280 and a shaking speed of 120 rpm at 30°C.

281 It was discovered that the maximum adsorption capacity increases from 20 minutes to 100
 282 minutes, and saturation occurs when the number of vacant sites reaches 100 minutes. During the
 283 first 100 minutes, the biosorption capacity increased from 70.8 mg/g to 124.7 mg/g due to the
 284 presence of ions that may precipitate the dye molecules.

285 (a)

286

287

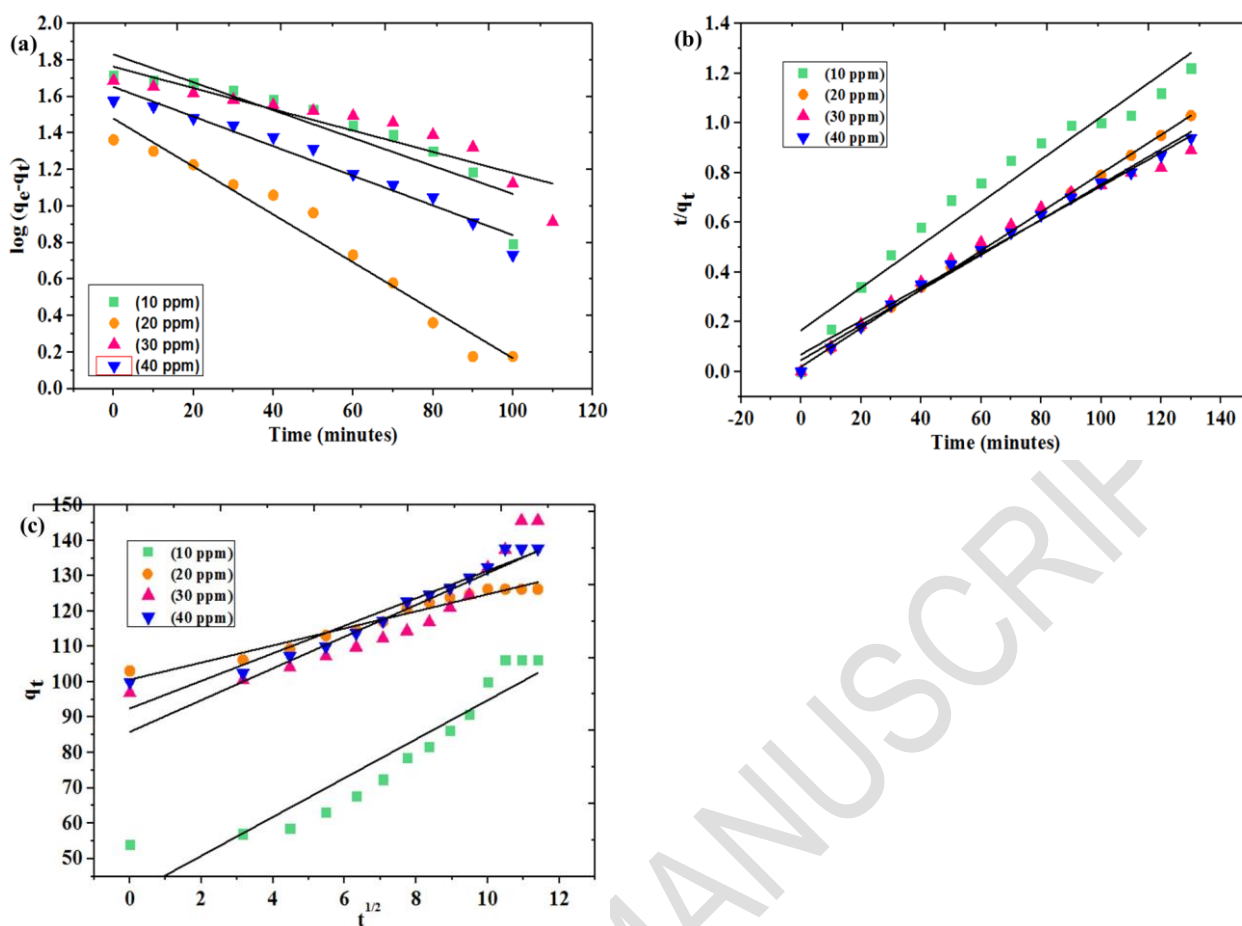


Fig. 9: (a) Pseudo first order kinetics (b) Pseudo second order kinetics (c) Intraparticle diffusion for the removal of Sunset yellow dye using MFPW adsorbent

The kinetic studies are helpful to understand the dynamics controlling mechanism of the adsorption process. The experimental data were analysed using three kinetic models (Fig. 9) such as pseudo-first-order, pseudo-second-order, and intraparticle diffusion to investigate the mechanism controlling dye adsorption onto mixed fruit peel waste. [Husseien, M *et al.*, 2007]

3.5.1. Pseudo-first-order model

An assumption in the pseudo-first-order kinetic model was that the rate of adsorbate removal changes with time. Thus, the adsorption capacity of the adsorbent changes. This is the linearized form of the pseudo-first-order kinetic equation.

$$\log(q_e - q_t) = \log q_e - \frac{k_1}{2.303} t$$

(9)

300

301 Pseudo-first-order model constant k_1 represents the adsorption capacity (mg/g) at equilibrium time
302 and the adsorption capacity (mg/g) at any point in time. [Husseien, M *et al.*, 2007]

303 3.5.2 Pseudo-second-order model

304 Electron-sharing between dye and adsorbent functional groups forms the basis of this model,
305 which assumes that adsorption occurs after chemisorption. The following is the formula:

$$\frac{t}{q_t} = \frac{1}{k_2 q_e^2} + \frac{t}{q_e} \quad (10)$$

306

307 Where k_2 indicate the rate constant of the pseudo-second-order kinetic model(g/mg min).

308 When determining k_2 , linear plots were drawn, and values of k_2 and q_e can be estimated from the
309 slope and intercept of the respective plot. [Husseien, M *et al.*, 2007]

310 3.5.3 Intraparticle diffusion model

311 The adsorption capacity changes with the square root of time in an intraparticle diffusion model, as
312 shown in the following equation.

$$q_t = k_{id} t^{0.5} + C_i \quad (11)$$

313

314 Where k_3 denotes the constant of intraparticle diffusion model and C indicate boundary layer
315 thickness (mg/g). This model helps to analyse the diffusion among the adsorbate and adsorption.
316 [A. Machrouhi *et al.*, 2017]

317 **Table 3: Estimated kinetic constants for adsorption of sunset yellow dye using MFPW**
318 **biosorbent.**

319

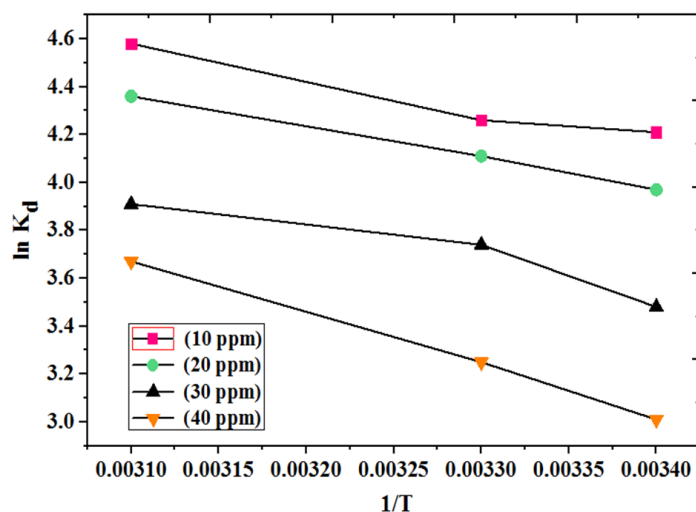
Kinetics	Parameters	10 ppm	20ppm	30ppm	40ppm
Pseudo first order kinetics	$Q_e(\text{mg/g})$	5.82	4.63	5.70	5.40
	$K_1(\text{min}^{-1})$	0.016	0.029	0.009	0.018
	R^2	0.83	0.97	0.88	0.96
Pseudo second order kinetics	$Q_e(\text{mg/g})$	125	142.85	166.67	142.85
	$K_2(\text{min}^{-1})$	0.003	0.0024	0.00052	0.0010
	R^2	0.95	0.999	0.977	0.993
Intraparticle diffusion model	$K_3(\text{mg/g min}^{1/2})$	5.5	2.416	4.489	3.896
	$C (\text{mg/g})$	39.81	100.6	85.87	92.50
	R^2	0.88	0.961	0.845	0.942

Table 3 lists the kinetic constants and R^2 values that were estimated. An R^2 value greater than 0.9 for pseudo-second-order kinetics that can be seen from the table. Predicted q_e from pseudo-second-order kinetics was in close agreement with the q_e measured. Electrostatic interactions were solely responsible for sunset yellow dye being adsorbed by fruit peel biosorbents, according to pseudo-second-order adsorption kinetics.

3.6 Effect of temperature on dye adsorption:

Sunset yellow dye adsorption was studied in the 30-50°C range, with an adsorbent dose of 2.0 g/100 ml, pH 3.0, and two hours of contact time. Fig. 10 represents the thermodynamics studies on SY FCF adsorption onto MFPW for various concentrations at different temperatures. And a summary of respective thermodynamic parameters ΔG° , ΔH° , and ΔS° are presented in Table 4. The Gibbs free energies (ΔG°) were found to be negative, indicating the adsorption of sunset yellow dye onto MFPW adsorbent to be both spontaneous and feasible, which does not require an external source for the process. Adsorption of the sunset yellow dye produced positive enthalpy change (ΔH°) values at various concentrations. Results were endothermic because the activation of dye molecules at the aligned sites of the fruit peels occurred as a result of an increase in temperature.

336 Adsorption sites in MFPW adsorbent that are empty become more and more attractive to anions
 337 with increasing temperature. The positive values of entropy change (ΔS°) indicated less randomness
 338 in their structural arrangement. [Olu-Owolabi *et al.*, 2010]



342 Fig. 10: **Thermodynamic** studies for the removal of Sunset yellow dye using MFPW adsorbent

343 **Table 4 : Thermodynamic parameters for ST FCF adsorption using MFPW adsorbent**

Co(mg/L)	T(K)	ΔG° (KJ/mol)	ΔH° (KJ/mol)	ΔS° (KJ/mol)	R^2
10	303	-24.347	24.617	0.163	0.95
	313	-26.621			
	323	-28.258			
20	303	-23.725	24.755	0.16	0.99
	313	-25.325			
	323	-26.925			
30	303	-21.117	25.848	0.155	0.90
	313	-22.667			
	323	-24.217			
40	303	-18.751	41.849	0.2	0.99
	313	-20.751			

	323	-22.751			
--	-----	---------	--	--	--

344

345 **3.7. Comparison of different adsorbents with mixed fruit peel adsorbent for the removal of**
346 **sunset yellow:**

347 The maximum adsorption capacity for removing SY FCF dye using MFPW was compared
348 with other such adsorbents. And Table 5 summarises the comparison of maximum adsorption
349 capacities for the removal of sunset yellow FCF dye using various fruit peel waste. Mixed Fruit peel
350 waste adsorbent has a higher adsorption capacity (200 mg/g) for sunset yellow FCF dye uptake than
351 the other adsorbents, which provides the surface area sites with well-developed pores for the
352 adsorption of dye **Table 5: Comparison of maximum adsorption capacity of sunset yellow dye**
353 **using fruit peel biosorbent with previous studies.**

Adsorbent	Adsorbate	Q _{max} (mg/g)	Reference
Treated fruit waste	Rhodamine B and methylene blue	34.48 35.71	Parimaladevi, P <i>et al.</i> , 2011
Pomegranate peel activated carbon	Remazol brilliant blue reactive dye	370.86	Ahmad, Mohd Azmier <i>et al.</i> , 2014
Green Pea Peels (<i>Pisum sativum</i>)	Methylene blue	163.94	Dod, Ramesh <i>et al.</i> , 2012
Coconut (<i>Cocos nucifera</i>) bunch waste	Methylene blue	70.92	Hameed, B. H <i>et al.</i> , 2008
Papaya seeds	Methylene blue	555.557	Hameed, B. H., 2009
Orange peel carbon	Direct yellow 12	75.76	Khaled, Azza <i>et al.</i> , 2009
Alligator weed activated	Sunset yellow	271	Kong, Qiang <i>et al.</i> , 2017

carbon			
Cadmium Sulfide Nanoparticle Loaded on Activated Carbon	Sunset yellow	83.3	Mosallanejad, N <i>et al.</i> , 2017
<i>Carica papaya</i> wood	Methylene blue	63.29	Nguyen <i>et al.</i> , 2020
Leaf residues of <i>Thymus numidicus</i> (RTN), <i>Origanum glandulosum</i> (ROG) and <i>Sapindus mukorossi</i> pericarp fibre (SMPF)	Methylene blue	24.2, 33.3 and 41	Djamila Youcef <i>et al.</i> , 2021
Positively charged biochar	Sunset yellow	74.07	Mahmoud et al., 2020
Zinc oxide nanorods loaded on activated carbon	Sunset yellow	142.85	Maghsoudi et al., 2015
Activated carbon derived from cassava sievate biomass	Sunset yellow	0.091	Chukwuemeka et al., 2021
Steam-activated carbon from malt bagasse	Sunset yellow	199.7	Lopes et al., 2021
Copper doped ZnS nanoparticles loaded on activated carbon	Sunset yellow	85.397	Agarwal et al., 2016
Mixed fruit peel waste	Sunset yellow	200	Present study

3.8 Cost evaluation and feasibility of MFPW

The preparation cost of any adsorbent is one of the most subtle characters to understand the economic feasibility of the industrial wastewater treatment. Hence, low-cost adsorbents with enhanced adsorptive properties are comparable to the available commercial adsorbents [Jayalakshmi and Jeyanthi 2022]. The raw materials here were collected as waste from the fruit

shop, which is discarded as garbage. Those wastes were collected at nil cost and hence required energy cost for the transportation charge and power consumption of chopping, shredding, drying and grinding of raw materials. Therefore, it was estimated to be 200INR/kg, and it was cost-effective compared to other adsorbents.

The preparation of MFP^W is simple since neither special equipment nor expertise handling is required. Also, it is biocompatible, sustainable and environmentally friendly since it is biomass waste. Furthermore, it is cost-effective and easy to scale up. These results altogether make the Mixed fruit peel waste a promising candidate for removing dye from an aqueous solution.

Conclusion:

A biosorbent made from prepared mixed fruit peel waste was used to remove the sunset yellow FCF dye successfully. According to the batch studies, the maximum adsorption capacity was 200 mg/g at pH 3.0, contact time of 100 minutes, adsorbent dose of 2.0g, and initial dye concentration of 40ppm. The regression coefficient for Langmuir isotherm data was more significant than or equal to 0.9, making it the best fit. The best adsorption kinetics are described by pseudo-second-order kinetics. The adsorption capacity of the mixed fruit peel waste adsorbent was higher than other such adsorbents. This study discovered that the highly exposed adsorption sites facilitate the adsorption mechanism. Therefore, it can be used as a cost-effective, eco-friendly and sustainable biosorbent for the efficient removal of textile dyes.

Acknowledgments:

The first author wishes to thank the Principal and Head of Industrial Biotechnology Department, Government College of Technology, Coimbatore, for providing facilities to carry out the current study.

References:

382 A. Machrouhi, M. Farnane, A. Elhalil, R. Elmoubarki, M. Abdenouni, S. Qourzal, H. Tounsadi and
 383 N. Barka(2017), Effectiveness of beetroot seeds and H₃PO₄ activated beetroot seeds for the
 384 removal of dyes from aqueous solutions. *Journal of Water Reuse and Desalination*. doi:
 385 10.2166/wrd.2017.034

386 Agarwal, S., Tyagi, I., Gupta, V. K., Dastkhooon, M., Ghaedi, M., Yousefi, F., & Asfaram, A.
 387 (2016). Ultrasound-assisted adsorption of Sunset Yellow CFC dye onto Cu doped ZnS
 388 nanoparticles loaded on activated carbon using response surface methodology based on
 389 central composite design. *Journal of Molecular Liquids*, 219, 332-340.

390 Ahmad, M. A., Eusoff, M. A., Adegoke, K. A., & Bello, O. S. (2021). Sequestration of methylene
 391 blue dye from aqueous solution using microwave assisted dragon fruit peel as
 392 adsorbent. *Environmental Technology & Innovation*, 24, 101917.

393 Ahmad, Mohd Azmier, Nur Azreen Ahmad Puad, and Olugbenga Solomon Bello (2014), Kinetic,
 394 equilibrium and thermodynamic studies of synthetic dye removal using pomegranate peel
 395 activated carbon prepared by microwave-induced KOH activation. *Water Resources and*
 396 *industry* 6: 18-35. <https://doi.org/10.1016/j.wri.2014.06.002>

397 Aksu, Z., and E. Balibek(2010),Effect of salinity on metal-complex dye biosorption by *Rhizopus*
 398 *arrhizus*, *Journal of environmental management* 91, no. 7 1546-1555.
 399 <https://doi.org/10.1016/j.jenvman.2010.02.026>

400 Almeida-Naranjo, C. E., Aldás, M. B., Cabrera, G., & Guerrero, V. H. (2021). Caffeine removal
 401 from synthetic wastewater using magnetic fruit peel composites: Material characterization,
 402 isotherm and kinetic studies. *Environmental Challenges*, 5, 100343.

403 Auta, M., and B. H. Hameed(2011),Optimized waste tea activated carbon for adsorption of
 404 Methylene Blue and Acid Blue 29 dyes using response surface methodology, *Chemical*
 405 *Engineering Journal* 175: 233-243. <https://doi.org/10.1016/j.cej.2011.09.100>

406 Barka, Noureddine, Ali Assabbane, Abederrahman Nounah, Larbi Laanab, and Yhya Aït
 407 Ichou(2009),Removal of textile dyes from aqueous solutions by natural phosphate as a new
 408 adsorbent, *Desalination* 235,no.1-3:264-275. <https://doi.org/10.1016/j.desal.2008.01.015>.

409 Bhatnagar, Amit, and A. K. Minocha(2009),Adsorptive removal of 2, 4-dichlorophenol from water
 410 utilizing Punica granatum peel waste and stabilization with cement, *Journal of hazardous*
 411 *materials* 168, no. 2-3: 1111-1117. <https://doi.org/10.1016/j.jhazmat.2009.02.151>.

412 Chukwuemeka-Okorie, H.O., Ekuma, F.K., Akpomie, K.G. et al. Adsorption of tartrazine and
 413 sunset yellow anionic dyes onto activated carbon derived from cassava sieveate
 414 biomass. *Appl Water Sci* 11, 27 (2021). <https://doi.org/10.1007/s13201-021-01357-w>

415 Djamila Youcef¹, Farida Fernane², Amel Hadj-ziane¹, Yasmine Messara²(2021). The kinetics
 416 and equilibrium sorption of methylene blue on plant residues in aqueous solution. *Euro-*
 417 *Mediterranean Journal for Environmental Integration* 6:59 [https://doi.org/10.1007/s41207-](https://doi.org/10.1007/s41207-021-00269-0)
 418 [021-00269-0](https://doi.org/10.1007/s41207-021-00269-0).

419 Dod, Ramesh, Goutam Banerjee, and S. Saini(2012). "Adsorption of methylene blue using green
 420 pea peels (*Pisum sativum*): A cost-effective option for dye-based wastewater
 421 treatment." *Biotechnology and Bioprocess Engineering* 17, no. 4: 862-874.
 422 <https://doi.org/10.1007/s12257-011-0614-5>

423 Garba, Z.N., Zhou, W., Zhang, M., Yuan, Z(2019), A review on the preparation, characterization
 424 and potential application of perovskites as adsorbents for wastewater treatment,
 425 *Chemosphere*, doi: <https://doi.org/10.1016/j.chemosphere.2019.125474>.

426 Garg VK , Gupta R , Yadav AB , Kumar R(2003) . Dye removal from aqueous solution by
 427 adsorption on treated sawdust. *Bioresour Technol*;89:121–4 .
 428 [https://doi.org/10.1016/S0960-8524\(03\)00058-0](https://doi.org/10.1016/S0960-8524(03)00058-0)

429 Georgin, J., da Boit Martinello, K., Franco, D. S., Netto, M. S., Piccilli, D. G., Yilmaz, M., Luis FO
 430 Silva, and Guilherme L. Dotto, (2021). Residual Peel of Pitaya Fruit (*Hylocereus undatus*)

431 as a Precursor to Obtaining an Efficient Carbon-based Adsorbent for the Removal of
 432 Metanil Yellow Dye From Water. *Journal of Environmental Chemical Engineering*,
 433 107006.

434 Gupta, Shubham A., Yamy Vishesh, N. Sarvshrestha, Adarsh S. Bhardwaj, Prince A. Kumar, Niraj
 435 S. Topare, Sunita Raut-Jadhav, Shantini A. Bokil, and Anish Khan(2021). "Adsorption
 436 isotherm studies of Methylene blue using activated carbon of waste fruit peel as an
 437 adsorbent." *Materials Today: Proceedings* .

438 Hameed, B. H(2009). "Evaluation of papaya seeds as a novel non-conventional low-cost adsorbent
 439 for removal of methylene blue." *Journal of Hazardous materials* 162, no. 2-3: 939-944.
 440 <https://doi.org/10.1016/j.jhazmat.2008.05.120>

441 Hameed, B. H., D. K. Mahmoud, and A. L. Ahmad(2008). "Equilibrium modeling and kinetic
 442 studies on the adsorption of basic dye by a low-cost adsorbent: Coconut (Cocos nucifera)
 443 bunch waste." *Journal of hazardous materials* 158, no. 1: 65-72.
 444 <https://doi.org/10.1016/j.jhazmat.2008.01.034>

445 Hejun Gao^{a,b}, Yun Wang^c, Liqiang Zheng^a(2013). Hydroxyl-functionalized ionic liquid-based cross-
 446 linked polymer as highly efficient adsorbent for anionic azo dyes removal. *Chemical*
 447 *Engineering Journal* 234 372–379. <https://doi.org/10.1016/j.cej.2013.08.078>

448 Hossain, N., Bhuiyan, M. A., Pramanik, B. K., Nizamuddin, S., & Griffin, G. (2020). Waste
 449 materials for wastewater treatment and waste adsorbents for biofuel and cement supplement
 450 applications: a critical review. *Journal of Cleaner Production*, 255, 120261.
 451 <https://doi.org/10.1016/j.jclepro.2020.120261>

452 Hussain, Sajjad, Zia Ullah, Saima Gul, Rozina Khattak, Nida Kazmi, Fozia Rehman, Sabir Khan,
 453 Khalid Ahmad, Muhammad Imad, and Adnan Khan(2016). "Adsorption characteristics of
 454 magnesium-modified bentonite clay with respect to acid blue 129 in aqueous media." *Polish*

455 *Journal of Environmental Studies* 25, no. 5: 1947-1953.
 456 <https://doi.org/10.15244/pjoes/62272>

457 Husseien, M., A. A. Amer, Azzar El-Maghraby, and Nahla A. Taha(2007). "Utilization of barley
 458 straw as a source of a activated carbon for removal of methylene blue from aqueous
 459 solution." *Journal of Applied Sciences Research* 3, no. 11: 1352-1358.

460 Idris, Mohd Nazri, Zainal Arifin Ahmad, Mohd Azmier Ahmad, Nazwin Ahmad, and Shamsul
 461 Kamal Sulaiman(2011). "Optimization of process variables for malachite green dye removal
 462 using rubber seed coat based activated carbon." *International Journal of Engineering &*
 463 *Technology* 11, no. 1: 234-240.

464 Jayalakshmi, R., & Jeyanthi, J. (2021). Dynamic modelling of Alginate-Cobalt ferrite
 465 nanocomposite for removal of binary dyes from textile effluent. *Journal of Environmental*
 466 *Chemical Engineering*, 9(1), 104924. <https://doi.org/10.1016/j.jece.2020.104924>

467 Jayalakshmi, R., Jeyanthi, J., & Sidhaarth, K. A. (2022). Versatile Application of Cobalt Ferrite
 468 Nanoparticles for the Removal of Heavy Metals and Dyes from Aqueous
 469 Solution. *Environmental , Nanotechnology, Monitoring & Management*, 17, 100659.

470 Khaled, Azza, Ahmed El Nemr, Amany El-Sikaily, and Ola Abdelwahab(2009),Treatment of
 471 artificial textile dye effluent containing Direct Yellow 12 by orange peel carbon."
 472 *Desalination* 238, no. 1-3 210-232. <https://doi.org/10.1016/j.desal.2008.02.014>

473 Khaskheli M.I., Chandio Z.A., Khan S., Khokhar F.M., Memon A.G., Jatoi W.B., Khokhar L.A.K.,
 474 and Shahani N.K. (2021), The utilization of okra leaves as an agricultural waste for the
 475 removal of As(III) and As(V), *Global NEST Journal*, 23(2), 257-264.

476 Kong, Qiang, Qun Liu, MingSheng Miao, YuZhen Liu, QingFeng Chen, and ChangSheng
 477 Zhao(2017): "Kinetic and equilibrium studies of the biosorption of sunset yellow dye by
 478 alligator weed activated carbon." *Desalination and Water Treatment* 66 ,281-290.

479 Lim, L. B., Priyantha, N., Latip, S. A. A., Lu, Y. C., & Mahadi, A. H. (2020). Converting
 480 *Hylocereus undatus* (white dragon fruit) peel waste into a useful potential adsorbent for the
 481 removal of toxic Congo red dye. *Desalin. Water Treat*, 185, 307-317. doi:
 482 10.5004/dwt.2020.25390

483 Lopes, G. K., Zanella, H. G., Spessato, L., Ronix, A., Viero, P., Fonseca, J. M., ... & Almeida, V. C.
 484 (2021). Steam-activated carbon from malt bagasse: Optimization of preparation conditions
 485 and adsorption studies of sunset yellow food dye. *Arabian Journal of Chemistry*, 14(3),
 486 103001.

487

488 Mall, Indra D., Vimal C. Srivastava, and Nitin K. Agarwal(2006). "Removal of Orange-G and
 489 Methyl Violet dyes by adsorption onto bagasse fly ash—kinetic study and equilibrium
 490 isotherm analyses." *Dyes and pigments* 69, no. 3: 210-223.
 491 <https://doi.org/10.1016/j.dyepig.2005.03.013>.

492 Mahmoud, M. E., Abdelfattah, A. M., Tharwat, R. M., & Nabil, G. M. (2020). Adsorption of
 493 negatively charged food tartrazine and sunset yellow dyes onto positively charged
 494 triethylenetetramine biochar: Optimization, kinetics and thermodynamic study. *Journal of*
 495 *Molecular Liquids*, 318, 114297.

496 Mosallanejad, N., and A. Arami(2012): "Kinetics and isotherm of sunset yellow dye adsorption on
 497 cadmium sulfide nanoparticle loaded on activated carbon." 31-40.

498 Nguyen, Thi Nhu Ngoc, Thi Thanh Hang Huynh, and Thi Hien To(2020). "Removal of methylene
 499 blue from simulated wastewater by *Carica papaya* wood biosorbent." *Vietnam Journal of*
 500 *Science, Technology and Engineering* 62, no. 4: 8-17.
 501 <https://vietnamscience.vjst.vn/index.php/VJSTE/article/view/366/251>

502 Olu-Owolabi, Bamidele I., and Emmanuel I. Unuabonah(2010):. "Kinetic and thermodynamics of
 503 the removal of Zn^{2+} and Cu^{2+} from aqueous solution by sulphate and phosphate-modified
 504 Bentonite clay." *Journal of hazardous materials* 184, no. 1-3, 731-738.
 505 <https://doi.org/10.1016/j.jhazmat.2010.08.100>

506 Parimaladevi, P., and V. Venkateswaran(2011):. "Adsorption of cationic dyes (rhodamine B and
 507 methylene blue) from aqueous solution using treated fruit waste." *J. Appl. Technol. Environ.*
 508 *Sanit* ,1 285-293.

509 Ramalingam, R. J., Sivachidambaram, M., Vijaya, J. J., Al-Lohedan, H. A., & Muthumareeswaran,
 510 M. R. (2020). Synthesis of porous activated carbon powder formation from fruit peel and
 511 cow dung waste for modified electrode fabrication and application. *Biomass and*
 512 *Bioenergy*, 142, 105800.

513 Rangabhashiyam S , Sujata Lata , Balasubramanian P (2017), Biosorption characteristics of
 514 methylene blue and malachite green from simulated wastewater onto Carica papaya wood
 515 biosorbent, *Surfaces and Interfaces* <https://doi.org/10.1016/j.surfin.2017.09.011>

516 Ranjithkumar, V., S. Sangeetha, and S. Vairam(2014):. "Synthesis of magnetic activated carbon/ α -
 517 Fe_2O_3 nanocomposite and its application in the removal of acid yellow 17 dye from
 518 water." *Journal of hazardous materials* ,273 127-135.
 519 <https://doi.org/10.1016/j.jhazmat.2014.03.034>.

520 Rebitanim, N. Z., Ghani, W. A. W. A. K., Mahmoud, D. K., Rebitanim, N. A., & Salleh, M. A. M.
 521 (2012). Adsorption capacity of raw empty fruit bunch biomass onto methylene blue dye in
 522 aqueous solution. *Journal of Purity, Utility Reaction and Environment*, 1(1), 45-60.

523 Sahu, S., Pahi, S., Sahu, J. K., Sahu, U. K., & Patel, R. K. (2020). Kendu (*Diospyros melanoxylon*
 524 Roxb) fruit peel activated carbon—an efficient bioadsorbent for methylene blue dye:
 525 equilibrium, kinetic, and thermodynamic study. *Environmental Science and Pollution*
 526 *Research*, 27(18), 22579-22592. <https://doi.org/10.1007/s11356-020-08561-2>

527 Shoukat, Sidra, Haq Nawaz Bhatti, Munawar Iqbal, and Saima Noreen(2017):. "Mango stone
528 biocomposite preparation and application for crystal violet adsorption: a mechanistic
529 study." *Microporous and Mesoporous Materials* 239 180-189.
530 <https://doi.org/10.1016/j.micromeso.2016.10.004>

531 Solangi, N. H., Kumar, J., Mazari, S. A., Ahmed, S., Fatima, N., & Mujawar, N. M. (2021).
532 Development of fruit waste derived bio-adsorbents for wastewater treatment: a
533 review. *Journal of Hazardous Materials*, 125848.

534 Sun, Yong, and Paul A. Webley. (2010)"Preparation of activated carbons from corncob with large
535 specific surface area by a variety of chemical activators and their application in gas
536 storage." *Chemical Engineering Journal* 162, no. 3: 883-892.
537 <https://doi.org/10.1016/j.cej.2010.06.031>

538 Wong, S., Ngadi, N., Inuwa, I. M., & Hassan, O. (2018). Recent advances in applications of
539 activated carbon from biowaste for wastewater treatment: a short review. *Journal of Cleaner
540 Production*, 175, 361-375.

541 Xiaoduo Liu^a, Jiefu Tiana^b, Yuanyuan Li^a, Ningfei Suna, Shu Mia,^c, Yong Xiea,* , Ziyu Chen,
542 (2019)Enhanced dyes adsorption from wastewater via Fe₃O₄ nanoparticles functionalized
543 activated carbon. *Journal of Hazardous Materials*, Volume 373, 5, Pages 397-
544 407.<https://doi.org/10.1016/j.jhazmat.2019.03.103>.

545 Yonggang Liu^{a,b}, Yoshihisa Ohko^{b,*}, Ruiqin Zhang^c, Yingnan Yang^a, Zhenya Zhang^a (2010)
546 Degradation of malachite green on Pd/WO₃ photocatalysts under simulated solar light.
547 *Journal of Hazardous Materials* 184, 386–391.
548 <https://doi.org/10.1016/j.jhazmat.2010.08.047>.

549 Yu Zhiyong^a, Wang Wenhua^b, Song Lin^c, Lu Liqin^a, Wang Zhiyin^d, Jiang Xuanfeng^a, Dong
550 Chaonan^a, Qiu Ruiying^a(2013). Acceleration comparison between Fe²⁺/H₂O₂ and CO²⁺/oxone for
551 decolouration of azo dyes in homogeneous systems. *Chemical Engineering Journal* 234 475–483.

552 DOI: [10.1016/j.cej.2013.08.013](https://doi.org/10.1016/j.cej.2013.08.013)Zhifeng Jiang, Jimin Xie*, Deli Jiang, Zaoxue Yan, Junjie Jing,
553 Dong Liu(2014); Enhanced adsorption of hydroxyl contained/anionic dyes on non functionalized
554 Ni@SiO₂ core-shell nanoparticles: Kinetic and thermodynamic profile.Applied Surface
555 Science,Volume 292, 15 Pages 301-310.<https://doi.org/10.1016/j.apsusc.2013.11.136>

ACCEPTED MANUSCRIPT